Real-Time Wavelet Based Blur Estimation on Cell BE platform

Nemanja Lukić[a], Ljiljana Platiša[b], Aleksandra Pižurica[b], Wilfried Philips[b] and Miodrag Temerinac[a]
[a]Novi Sad University, Faculty of Technical Sciences, Trg Dositeja Obradovića 6, Novi Sad, Serbia
[b]Ghent University, Department of Telecommunications and Information Processing
TELIN-IPI-IBBT, Sint-Pietersnieuwstraat 41, Gent, Belgium

ABSTRACT

We propose a real-time system for blur estimation using wavelet decomposition. The system is based on an emerging multi-core microprocessor architecture (Cell Broadband Engine, Cell BE) known to outperform any available general purpose or DSP processor in the domain of real-time advanced video processing solutions. We start from a recent wavelet domain blur estimation algorithm which uses histograms of a local regularity measure called average cone ratio (ACR). This approach has shown a very good potential for assessing the level of blur in the image yet some important aspects remain to be addressed in order for the method to become a practically working one. Some of these aspects are explored in our work. Furthermore, we develop an efficient real-time implementation of the novelty metric and integrate it into a system that captures live video. The proposed system estimates blur extent and renders the results to the remote user in real-time.

Keywords: blur estimation, image quality, wavelets, real-time, multi-core, Cell BE

1. INTRODUCTION

The appearance of high definition (HD) digital content provides more impressive visual sensation by offering higher level of details compared to the standard definition. At the same time, the amount of data to be transmitted and processed has significantly increased which amplifies the urge for high processing power. Given the high demands for both capacity and speed, it needs no debate that the techniques to guarantee the quality of service (QoS) are of utmost importance. In this respect, the quality of video material has to be evaluated in real-time for live streams or even faster for offline content.

One of the most common causes of image quality distortion is image blur which is inevitably introduced not only at the point of image acquisition but also during the iterations of image processing and broadcasting. Consequently, blur estimation is high among priorities of image quality analysis. Different types of blur include linear motion blur, atmospheric turbulence blur and uniform focal, or out-of-focus blur. In this work, we will consider focal blur modeled by a Gaussian function as a conventional blur that often occurs in images.

A large and growing body of literature has investigated blur estimation techniques. Many of the existing methods strongly depend on the results of edge detection in the degraded image. For example, Rooms *et al*. [1], Tong *et al*. [2] and Lin *et al*. [3] use the ability of wavelet transform to detect location of the edges. Marziliano *et al*. [4], and more recently Wang *et al*. [5] make use of rather simple techniques of Canny or Sobel filtering to determine the edge positions. These edge detection techniques are affected by the level of noise in the degraded image. Hence, the related blur metrics are not only sensitive to edge detection but to noise as well. Alternatively, Hu *et al*. [6] proposed a new blur estimation method based on the difference between two re-blurred versions of an image. To its advantage, this metric involves no computationally demanding transformations and needs no edge detection thus the cost of data processing is significantly lower compared to the aforementioned methods. Nevertheless, similar to the others, Hu's metric also demonstrates high dependency on the content and fails to discriminate between higher levels of blur.

Recently, some of the authors of this paper have proposed a metric named CogACR [7] that is based on the wavelet transform and local regularity measure named average cone ratio (ACR) [8]. Tested for artificaly blurred natural scene images, CogACR demonstrates high level of discrimination between different levels of blur and for a significant range of blurrines in the image. Especially, CogACR is highly robust to noise which is one of the most common types of degradation in video sequences. Similar to other existing methods, however, CogACR as it is currently defined, suffers from content sensitivity and requires further investigation in that direction. Overall, despite its computational complexity

Wavelet Applications in Industrial Processing VII, edited by Frédéric Truchetet, Olivier Laligant,
Proc. of SPIE-IS&T Electronic Imaging, SPIE Vol. 7535, 75350C · © 2010 SPIE-IS&T
CCC code: 0277-786X/10/$18 · doi: 10.1117/12.839501

and content sensitivity, the results presented in [7] indicate high potentials of CogACR metric. Therefore, we chose this method for our real-time implementation. Further on, the implementation is used to verify the conclusions from [7] for real live HD content and evaluate the potentials for using the CogACR metric in actual real life applications.

Considering HD demand for high data throughput, we select to use Cell Broadband Engine (Cell BE) architecture for digital signal processing. This architecture proved to perform very efficiently in such cases. Moreover, it offers better solutions for the real-time advanced video processing than any other available general purpose or DSP processor based platform. Importantly, Cell BE architecture offers processing power comparable to FPGA DSP modules [9] while preserving speed and flexibility of the software development. Even so, to achieve best results, certain hardware constraints need to be taken into account when programming Cell BE. These include memory alignment, limited cache memory size, vector nature of processing elements and special inter-core synchronization techniques. When these constraints are satisfied, the theoretical peak performance can easily be achieved. Here, the major challenge of CogACR implementation, hereafter referred to as CellCogACR (CCACR), is the implementation of wavelet transform. To date, a number of different techniques for implementing the critically sampled discrete wavelet transform (DWT) using the Cell BE architecture have been introduced [10], [11]. To the authors knowledge, the Cell BE implementations of overcomplete wavelet transforms used in CogACR metric and especially blur estimation methods have not been studied.

In this paper, we propose an efficient implementation of a novelty wavelet based CogACR metric on the Cell BE based platform, CCACR. Our results show that the implementation is able to achieve real-time performance for HD input stream (1080i, 60 Hz). Furthermore, we extend the existing video quality assessment system [12] with CogACR metric and test the new system's behavior with a commercially available HD Set Top Box (STB). We used Sky+HD box from British Sky Broadcasting.

The paper is organized as follows. In Section 2 provides an overview of selected wavelet based blur estimation method and compares it with existing methods. Destination platform is described in Section 3. Section 4 presents optimization techniques used to achieve real-time performance while implementing selected method on destination platform. Section 5 gives overview of the achieved experimental results in terms of processing time of the optimized CogACR method and compares it with achieved results with other methods. Section 6 provides overview of the proposed system for real-time blur estimation. Conclusions can be found in Section 7.

2. WAVELET BASED COGACR METHOD

The main idea of the CogACR metric [7] is to estimate blur from the histogram of the local regularity estimates in the wavelet domain. The method employs the so-called *average cone ratio* (ACR) metric which is a noise-robust estimate of the local Lipschitz exponent. ACR is defined by Pižurica *et al*. [8] as a quantity which characterizes joint expansion of the magnitudes of wavelet coefficients inside a cone of influence which is centered at the given spatial position. It was shown in [8] that the ACR is a good estimate of the local Lipschitz exponent α, in particular an estimate of Lipschitz $\alpha + 1$. Moreover, the study proved that the ACR measure is insensitive to noise. Since this metric is highly insensitive to noise and depends on the regularity of the edges, it can measure blur. In [7], it was proposed to use the *center of gravity* of the ACR (hence the name CogACR) as a measure of blurriness. Furthermore, it was shown that the proposed blur metric is valid both in case where the reference image is available and in case where it is not available.

For testing purposes, we used Kodak Test Images [13] transformed to the grayscale and cropped to the size of 512x512 pixels. The images are blurred with Gaussian blur with radius r varied in the range of 0.25 pixels to 5.0 pixels with the uniform step of 0.25, $r=\{r \in R: r_k=0.25k, k=1,2,\ldots,20\}$. To create noisy images, Gaussian noise with variance of 25 was introduced.

In Fig 2 we compare performance of CogACR to Lin's metric [3]. We choose Lin's method for comparison as this method is also wavelet based method that uses ratio of the wavelet coefficients at different wavelet scales to estimate blur level in input image. The main differences between CogACR and Lin's method's is that CogACR uses non-decimated wavelet transform and takes into account cone of influence which is centered at the given spatial position while Lin's method calculates ratio on point wise basis. The results shown in Fig 2 clearly show that CogACR is more sensitive to the level of blur and able to detect higher levels of blur with more confidence.

Further on, in Fig 3 we compare the performance of CogACR metric to the other two recent ones, Hu's metric [6] and Tong's metric [2]. We chose Hu's method for comparison because this blur estimation method is not wavelet based and

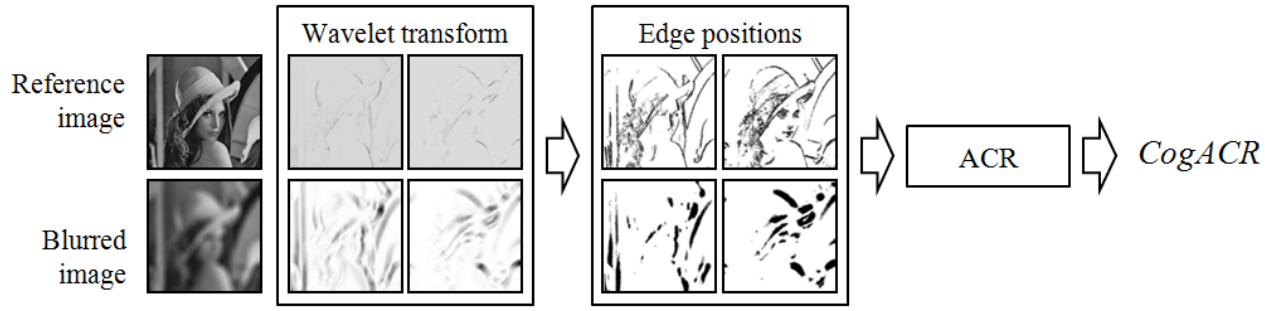

Fig 1. A flowchart of the CogACR metric. The ACR is calculated from the wavelet coefficients at the estimated edge positions and the center of gravity of ACR (CogACR) is used as a blur measure. For more details, see [7].

thus not computationally desired as other wavelet based methods. Tong's metric is chosen as example of complex wavelet based method with promising results in blur estimation. We are comparing CogACR with these two methods in terms of both computational complexity and achieved results in estimation of blur. For behavior in blur estimation comparison we used same test images, and test environment as described in previous paragraphs. The results shown in Fig 3 prove that the CogACR is able to distinguish between different levels of blur with higher level of confidence than the referent methods while preserving very low noise sensitivity, especially in case of lower levels of blur. Both referent methods reach saturation for blur radius of 1.5 while for higher radius of blur the methods are practically insensitive. The comparison shown in Fig 2 and Fig 3 together with the results presented in [7] motivates our choice of CogACR metric.

Along with the aforementioned benefits of CogACR, in order to generate a practical method for out-of-focus blur estimation, further investigation is needed to resolve some of the drawbacks of the existing metric: an automated algorithm for mask selection in the phase of edge-detection, image classification in case where the degradation free image is not available (content sensitivity), and, quite general, options for further reducing computational intensity of the metric.

3. CELL BE ARCHITECTURE

Considering the complexity of the selected blur metric, hardware platform with high processing power is needed for real-time implementation. To fit these requirements, we chose Cell BE based hardware architecture [14]. This platform offers high processing power, even comparable with programmable hardware architectures like FPGA [9], as well as increased programming comfort, flexibility and speed (use of high level programming languages like C/C++). Cell BE is an architecture of multi-core microprocessors dedicated for distributed data processing. It is comprised of two types of processing cores: a general purpose Power Processing Element (PPE) and a dedicated DSP cores known as Synergistic Processing Elements (SPE). Fig 4 presents architecture of processor based on Cell Broadband Engine Architecture (CBEA).

The processor characteristics include multiple heterogeneous execution units (SPE and PPE processors), Single Instruction Multiple Data (SIMD) processing engines for parallel data processing, fast local store for smaller memory latency and a software managed cache for parallelization of data manipulation and acquisition process. As mentioned earlier, the Cell BE applications can achieve performance which is close to the theoretical peak performance assuming the specific hardware features are respected: memory alignment, limited cache memory, vector nature of SPE processor and special inter-core synchronization techniques. Cell BE based platform offers parallelism on three levels:

1. Parallelism on the *algorithmic* level (different video algorithms and/or different parts of image being processed can be simultaneously executed on different SPE cores).
2. Parallelism on *data processing* level (usage of SIMD instruction set enables processing of up to 16 data using single processor instruction).
3. Parallelism on *data acquisition* level (processing of data and data acquisition are fully asynchronous processes).

Combining these levels of parallelism, Cell BE based platform offers, in the ideal case, an average performance that is more than 100 times better than that of a platform based on general purpose processor with similar processor frequency.

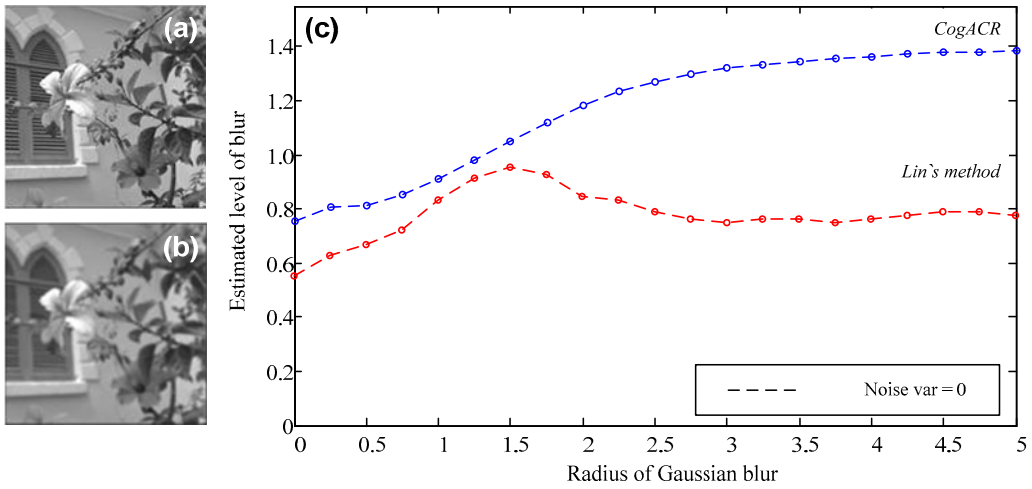

Fig 2. CogACR metric compared to Lin's metric. The results are obtained for test image Kodim07: (a) Degradation free image of 512x512 pixel size, (b) Degraded image with Gaussian blur of radius r=5, without noise, (c) CogACR metric for Gaussian blur with r= {0, 0.25, 0.5, … 5}.

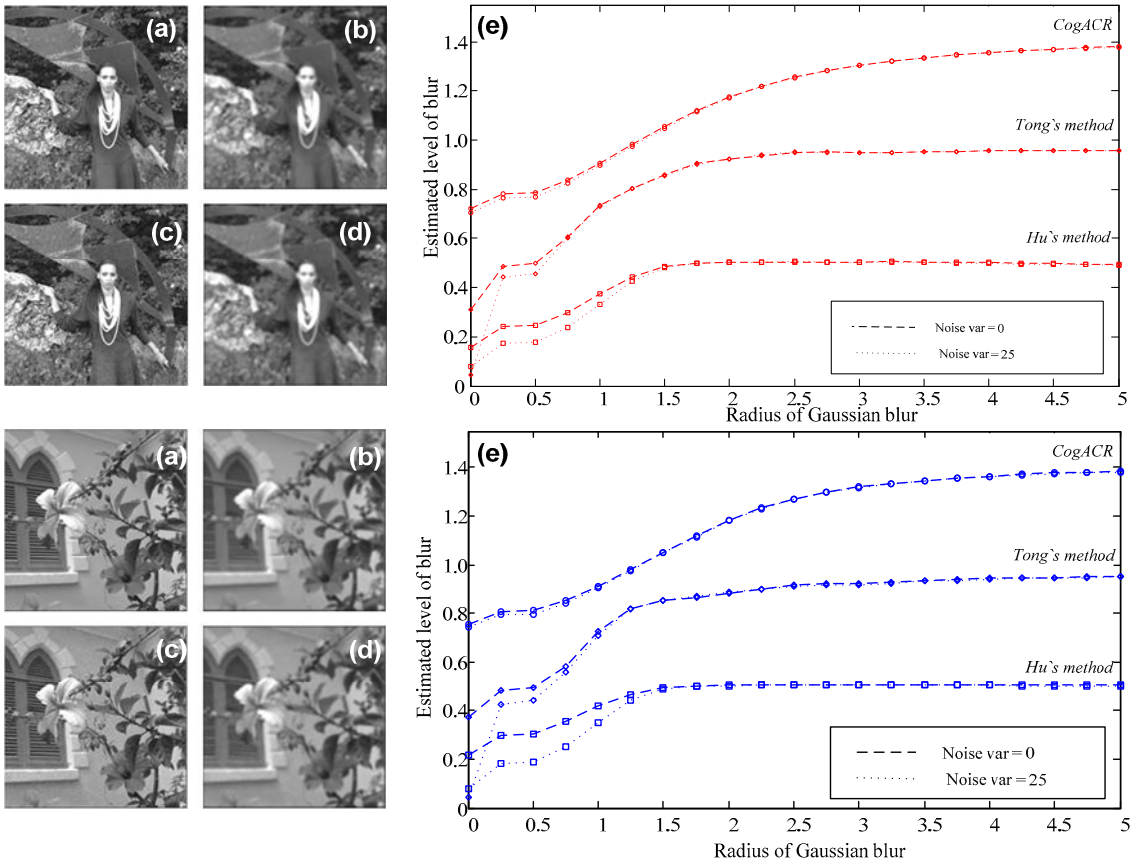

Fig 3. CogACR metric compared to Tong's metric and Hu's metric of blur. The results are obtained for test images Kodim07 and Kodim 18: (a) Degradation free image of 512x512 pixel size, (b) Degraded image with Gaussian blur of radius r=5, (c) Blur-free image with Gaussian noise, var = 25, (d) Degraded image with Gaussian blur (r=5) and Gaussian noise (var=25), (e) CogACR metric for Gaussian blur with r= {0, 0.25, 0.5, … 5}.

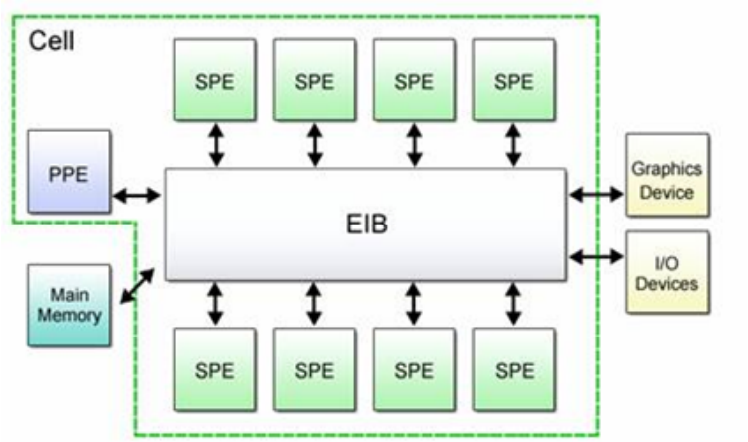

Fig 4. Architecture of a processor based on Cell BE architecture. Architecture consists of multiple heterogeneous execution units and those are: 1 general purpose PPE processor core and 8 dedicated DSP processing cores. Data throughput is guaranteed with fast Element Interconnect Bus (EIB) that connects cores with output peripherals and each other.

4. REAL-TIME IMPLEMENTATION ON CELL BE

In order to achieve real-time performance, implementation of CogACR metric needs to be adapted to take into account hardware specifications of Cell BE. To start with, the size of HD field (~2MB) exceeds limited cache size of SPE processors (256 KB) which caused implementation of line based memory buffers and double buffering techniques for image data acquisition from the main memory. Secondly, vector nature of SPE processors forced the use of SIMD instructions and adapting algorithm to SIMD processing in order to achieve most efficient performance.

4.1 Multi-core programming model

In general, two different models of multi-core programming exist on Cell BE architecture: PPE and SPE centric model [15]. In the former model, every SPE core is performing the entire processing chain but on a reduced amount of data (only part of the input image). In SPE centric model, each SPE processor is responsible for different processing steps and special synchronization mechanisms are needed. This method is preferred in situations when data cannot be easily divided into independent segments. Based on our experience, the former model outperforms the latter one in achieving real-time performance. Hence, we select PPE centric model for our implementation. In our work, the processing time is accelerated by dividing input image into horizontal stripes and assigning one SPE processor to every generated stripe, as illustrated in Fig 5. The results from all SPE processors are gathered on PPE core, and combined into the final measurement result. PPE core is also responsible for data acquisition and dividing of the input image into independent horizontal stripes.

4.2 The SIMD implementation of the non-decimated wavelet transform

As proposed in [8], an oversampled (non-decimated) cubic-spline wavelet transform is used for calculation of ACR. This wavelet filter bank uses floating point coefficients for both high and low pass filters. However, Cell BE processor is optimized for processing of the fixed point data types. Cell BE SIMD fixed point instructions can process 4, 8, or 16 operands depending on operand's bit length, while floating point instructions can only process 2 or 4 floating point numbers. These limitations are introduced with the fact that register bit length of SPE processor is 128 bits. For CogACR method only 3 bands are of interest at every wavelet scale: detailed images in LH and HL band for ACR calculation and LL band for calculation of the next wavelet scale. In [7] it is observed that CogACR method shows best results when ACR2-4 is used (wavelet scales from second to fourth).

Aiming to generate the most efficient implementation of the wavelet transform, floating point calculations had to be avoided. In order to transform the coefficients from floating to fixed point domain, they had to be multiplied by scalar value M, in our case M=8. By multiplying coefficients by factor M, detail images HL and LH on first scale had values M times grater than they should have, while LL values were M^2 times greater (due to the double low pass filtering on every

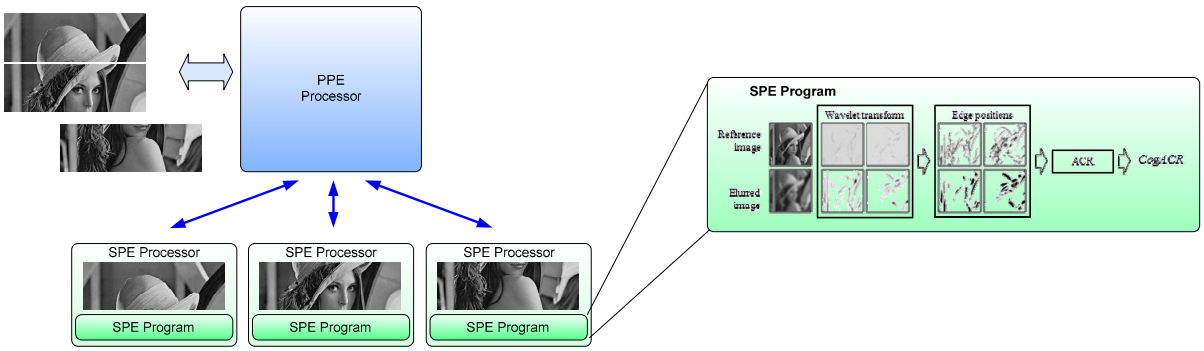

Fig 5. Cell BE multi-core programming model used for implementation of the CogACR. The enlarged part illustrates SPE program block diagram. This model is used when processing can be divided between multiple cores by dividing input data into blocks and allocating specific blocks of data to single core. For this model ne inter-core communication is needed.

pixel value). Consequently, the values of detail images on all scales are multiplied by factor $M^{2^{*}j+1}$, $j \in N$, $j \geq 0$, where j represents the scale. Clearly, to neutralize this effect of "trick" multiplications by M, after all wavelet scales are calculated, the coefficients from detail images have to be normalized by $M^{2^{*}j+1}$. Given the fact that fixed point instructions are multiple times faster than their floating point counterparts, it is better to do floating point only at the end of wavelet transformation instead of calculating all wavelet scales in floating point. Another advantage of using the fixed point data types for calculations is the fact that these data types can have different bit length (8, 16, 32 or 64 bit), while floating point data types are always either 32 or 64 bit in length. This practically means that one can use data type that has appropriate length according to the range of the data to be stored. This fact is illustrated in Fig 6 where different data types are used in different wavelet scales. First scale uses SIMD instructions that handle vectors comprised of sixteen 8 bit values (for 8 bit input video sequences, allowing parallelism on data level by processing 16 pixels in parallel), and output results to two vectors comprised of eight 16 bit values. Second scale of wavelet uses SIMD instructions that handle vectors comprised of eight 16 bit values (outputs from the first scale, allowing parallelism on data level by processing 8 pixels in parallel), and output results to four vectors each comprised of four 32 bit values. This allows wavelet implementation to be as efficient as possible, concerning instruction set being used. If we decided to use float point data types, maximum parallelism on the data level that we could expect is 4 (four 32 bit values fit into one 128 bit vector). The only exception is the fourth scale for which the LL wavelet coefficients are not calculated. This is due to the fact that our implementation makes use of only the first four wavelet scales and thus calculation of the LL band can be omitted.

5. EXPERIMENTAL RESULTS AND DISCUSSION

Fig 7 (a) depicts the processing times of the compared measures on a single SPE core. Expectedly, Hu's metric achieved the highest frame rate due to the fact that this method is not based on wavelet transform. Unlike CogACR, Tong's metric is based on decimated wavelet transform which attributes to its higher frame rate compared to CogACR.

In Fig 7 (b), the number of SPE cores needed for CogACR real-time performance is shown. Because all cores are running in parallel and no inter-core communication is needed, the achieved frame rate only depends on the time needed for the slowest core to complete its processing part. For the PAL HD signal (50 Hz) 2 SPE cores are adequate, but for the NTSC HD signal 3 SPE cores are needed. The deployment of PPE core is mandatory in both cases, because it is responsible for input data acquisition and collection and afterword combining of partial results from the used SPE cores.

Table 1 shows how different parallelism on data level can influence execution time of appropriate scale. Execution time expressed in milliseconds is approximately doubled with every ascending wavelet scale, due to the fact that parallelism on data level is reduced by 50% (fewer pixels can be processed in parallel, due to the minimum data length). The only exception is the fourth scale for which the LL wavelet coefficients are not even calculated. This is due to the fact that our implementation makes use of only the first four wavelet scales and thus calculation of the LL band can be omitted.

Table 2 shows code profiling of the CCACR for different input video resolution. Target resolution for the real-time performance is HD (1080i, 60Hz). The part of the algorithm that is the most computationaly expensive, around 38% of processor time, is wavelet transform with coefficient normalization. This result is expected due to the fact that CogACR

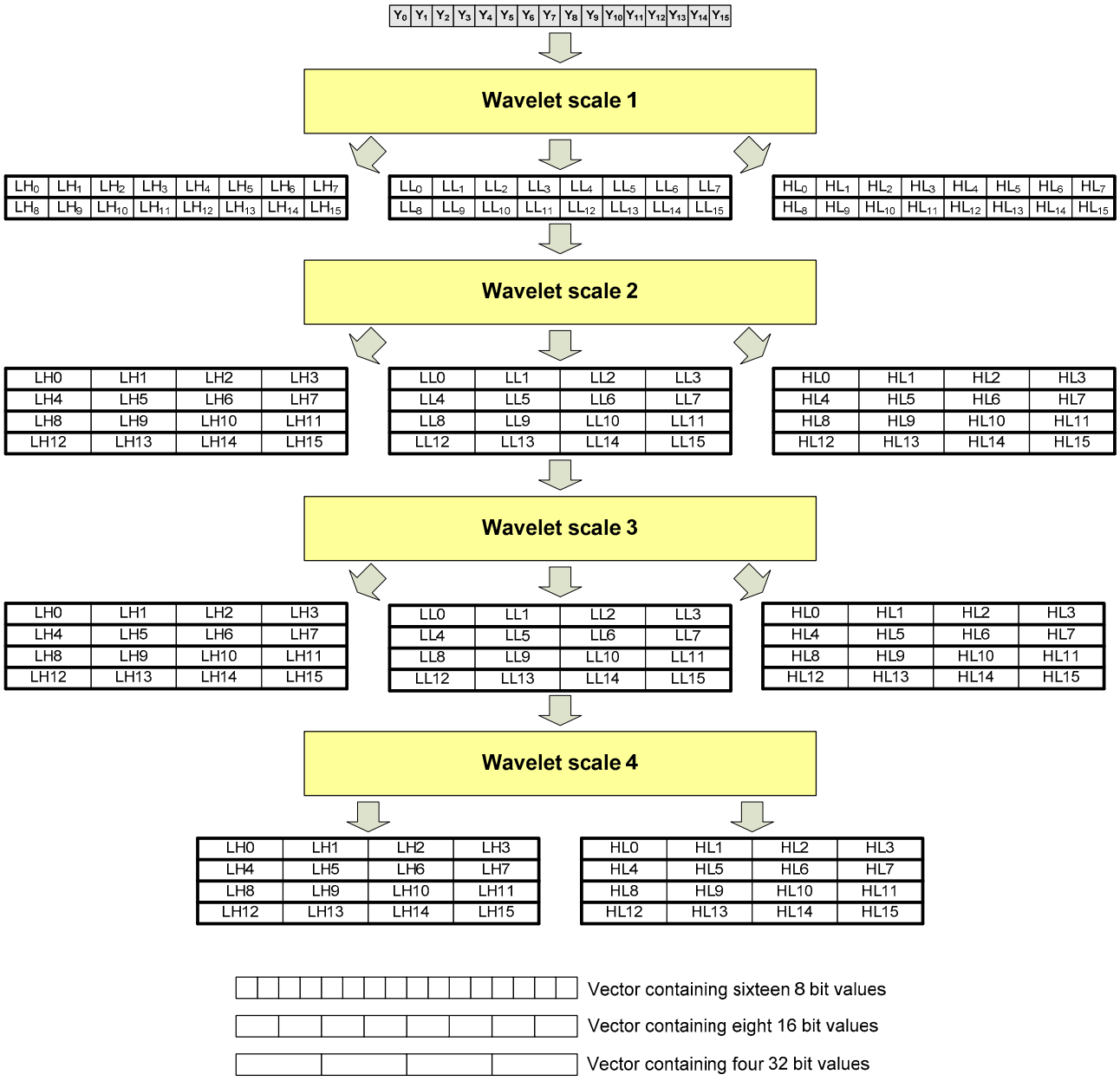

Fig 6. Block scheme of SIMD implementation of the non-decimated wavelet transform

uses non-decimated wavelet transform and that for our calculations we need first four wavelet scales (other metrics use fewer scales). As the results show, for target real-time performance (16.6 *ms*) several SPE cores will have to be employed. Core allocation will be addressed in later paragraphs.

We used the novel real-time implementation of CogACR metric to improve an existing platform for image quality estimation described in [12].

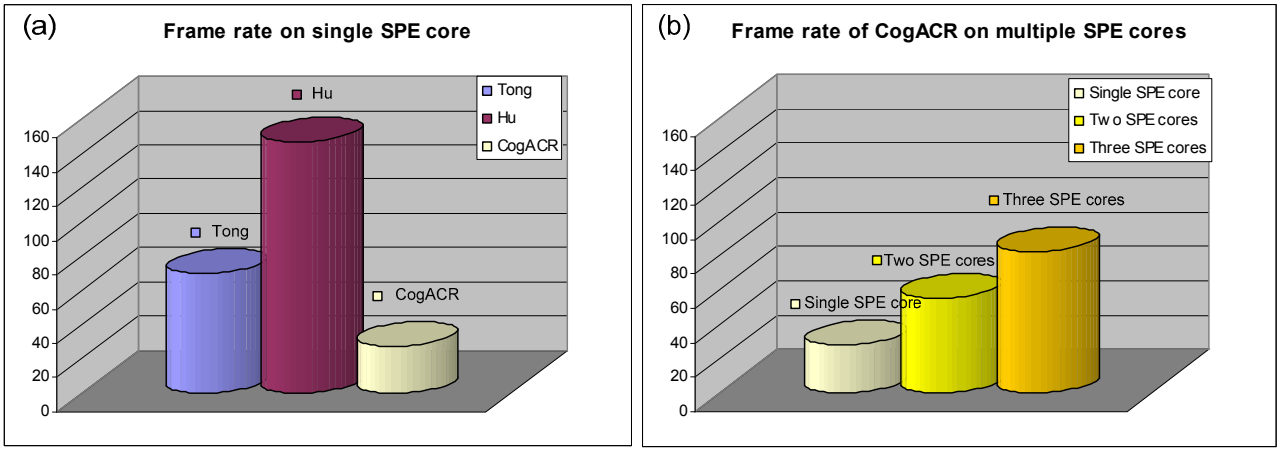

Fig 7. Cell BE implementation of CogACR metric compared to the implementation of Tong's and Hu's metric. (a) Frame rate on single SPE core (b) Frame rate of CogACR implementation when divided on multiple SPE cores

Table 1. Measured execution time needed for 4 different wavelet scales. The measurements are performed on a single SPE core. The values are given in milliseconds, *ms.*

Wavelet scale/Resolution	**1080i**	**720p**	**576i**	**480i**
1st scale	1.44	1.28	0.29	0.24
2nd scale	2.69	2.39	0.54	0.45
3rd scale	4.45	3.96	0.89	0.74
4th scale	1.19	1.06	0.24	0.20
First four scales	9.77	8.69	1.95	1.63

Table 2. Measured execution time needed for specific algorithmic parts of the optimized CogACR. Measurement is performed on single SPE core and illustrated in *ms*

Function/ Resolution	**1080i**	**720p**	**576p**	**480p**	**576i**	**480i**	**Overall contribution**
Wavelet	9.77	8.69	3.91	3.26	1.95	1.63	28.48%
Normalization	3.50	3.11	1.40	1.17	0.70	0.58	10.20%
ConesMagSumVertical	6.35	5.65	2.54	2.12	1.27	1.06	18.52%
RatioSectorRow	3.95	3.51	1.58	1.32	0.79	0.66	11.52%
ConesMagSumHorizontal	6.78	6.03	2.71	2.26	1.36	1.13	19.76%
RatioSectorRow	3.95	3.51	1.58	1.32	0.79	0.66	11.52%
All together	34.31	30.50	13.72	11.44	5.86	5.72	100.00%

6. THE PROPOSED REAL-TIME ENVIRONMENT

Fig 8 represents architecture of the real-time Video Quality Analysis (VQA) platform used in our study. This platform consists of three main components: capture device (network attached capture device, NACD), processing server (PS) and monitoring workstation (MW). Input of NACD is live video feed provided by an external source that can be either analog or digital, SD or HD (component, composite, S-Video, SDI or HDMI interface).

Captured data is streamed to PS using 1Gbps Ethernet connection. As the bandwidth required for transmission of raw video data of HD resolution at full frame rate exceeds the capability of the network, lossless compression of input video is applied. Lossless compression is used to avoid the introduction of new artifacts. In particular, the selected compression achieves an average compression ratio of 2.5. When this compression is applied on high definition video, generated bit rate never exceeds 500 Mbps. This throughput is comfortably below the theoretical physical limit of network in use (1 Gbps).

Video quality measurement is performed on PS in real-time. Measurement results, combined with downscaled preview of input video are sent to MW via LAN. MW may be dislocated, meaning that remote access to PS is possible via Internet. Frame rate and downscale factor of preview video depend on connection quality between PS and MW. Measurement results are always transmitted at same rate as input video. The system considers blocking, ringing and blurring artifacts. Existing blur estimation metric in this system distinguishes only three levels of blur degradation: good, intermediate and bad.

We substituted system's existing blurring measurement algorithm with the proposed real-time implementation of the CogACR metric. Fig 9 shows task allocation of the proposed real-time environment. In order to achieve real-time performance for live HD content (1080i, 60Hz) three SPE cores are reserved for CogACR. The system is tested and evaluated with commercially available STB. Results obtained when CogACR is used as blur estimation metric in this system indicate that we can detect more subtle gradations of blur extent, and this with more confidence. This enables differentiation of more subtle levels of blur degradation that consequently expands areas in which this system can be successfully employed, like assessment of medical images, digital panels, etc.

7. CONCLUSION

In this paper we proposed a real-time blur estimation system using wavelet decomposition, CCACR. We motivated the choice of CogACR as a blur metric showing its superior performance over related methods in terms of sensitivity, measurable range of blur levels and robustness to noise. The proposed system is based on IBM Cell BE multi-core microprocessor architecture.

Encouragingly, the results of our work suggest that even complex metric for blur estimation based on the non-decimated wavelet transform can be efficiently implemented on a commercially available processor and achieve real-time performance for HD input. Our implementation uses only part of the strength that Cell BE platform offers (3 out of 8 SPE cores are used for real-time performance). Moreover, we extended an existing video quality assessment platform with this metric and tested its performance with commercially available STB. Further research is ongoing in order to improve the existing CogACR metric, and thus the CCACR system.

REFERENCES

[1] Rooms, F., Pižurica, A., and Philips, W., "Estimating image blur in the wavelet domain," Proc. of the Fifth Asian Conference on Computer Vision (ACCV), pp. 210-215 (2002).

[2] Tong, H., Li, M., Zhang, H., and Zhang, C., "Blur detection for digital images using wavelet transform," Proc. ICME, 17-20 (2004).

[3] J. Lin, C. Zhang, Q. Shi, "Estimating the amount of defocus through a wavelet transform approach", Pattern Recognition Letters, v.25 n.4, p.407-411, March 2004

[4] Marziliano, P., Dufaux, F., Winkler, S., Ebrahimi, T. and Sa, G., "A no-reference perceptual blur metric," Proc. ICIP, 57-60 (2002).

[5] Wang, X., Tian, B., Liang, C. and Shi, D., "Blind Image Quality Assessment for Measuring Image Blur," Proc. CISP, vol. 1, 467-470 (2008).

[6] Hu, H., de Haan, G., "Low Cost Robust Blur Estimator", Proc. ICIP, pp. 617-620 (2006).
[7] Ilić, Lj.; Pižurica, A.; Vansteenkiste, E.; Philips, W. "Image blur estimation based on the average cone of ratio in the wavelet domain", Wavelet Applications in Industrial Processing VI, Volume 7248, San Jose, CA, USA (2009).
[8] Pižurica, A., Philips, W., Lemahieu, I. and Acheroy, M., "A Joint Inter- and Intrascale Statistical Model for Bayesian Wavelet Based Image Denoising," IEEE Trans. on Image Processing, vol. 11, no. 5, 545-557 (2002).
[9] Lukić, N., Papp, I., Marceta, Z., Ačanski, D., Temerinac, M., "Evaluation of CELL IBM platform regarding development of advanced real-time video algorithms", Proc. of the IEEE ICEST, pp. 407-410 (2008).
[10] Asahara, A.; Doi, M.; Mori, Y.; Nishiyama, H.; Nakano, H, „Cell-Broadband-Engine-Based Realtime Wavelet Decomposition for HDTV Video Images and Beyond", Proc. Of the IEEE ICME, pp. 445 – 448 (2006).
[11] Schiller A., Sutmann, G., Yang, L., "A Fast Wavelet Based Implementation to Calculate Coulomb Potentials on the Cell/B.E.", Proc. of the 10th IEEE HPCC, vol. 00, pp. 162-168 (2008).
[12] Papp I., Lukić N., Marčeta M., Teslić N., Schu M., "Real-time Video Quality Assessment Platform", 27th International Conference on Consumer Electronics, Las Vegas, USA (2009).
[13] Kodak Test Images, http://r0k.us/graphics/kodak/
[14] "Cell Broadband Engine Architecture", IBM (2007).
[15] "Cell Broadband Engine Architecture C/C++ Language Extensions for CBEA", Cell SDK 2.1, IBM (2007).

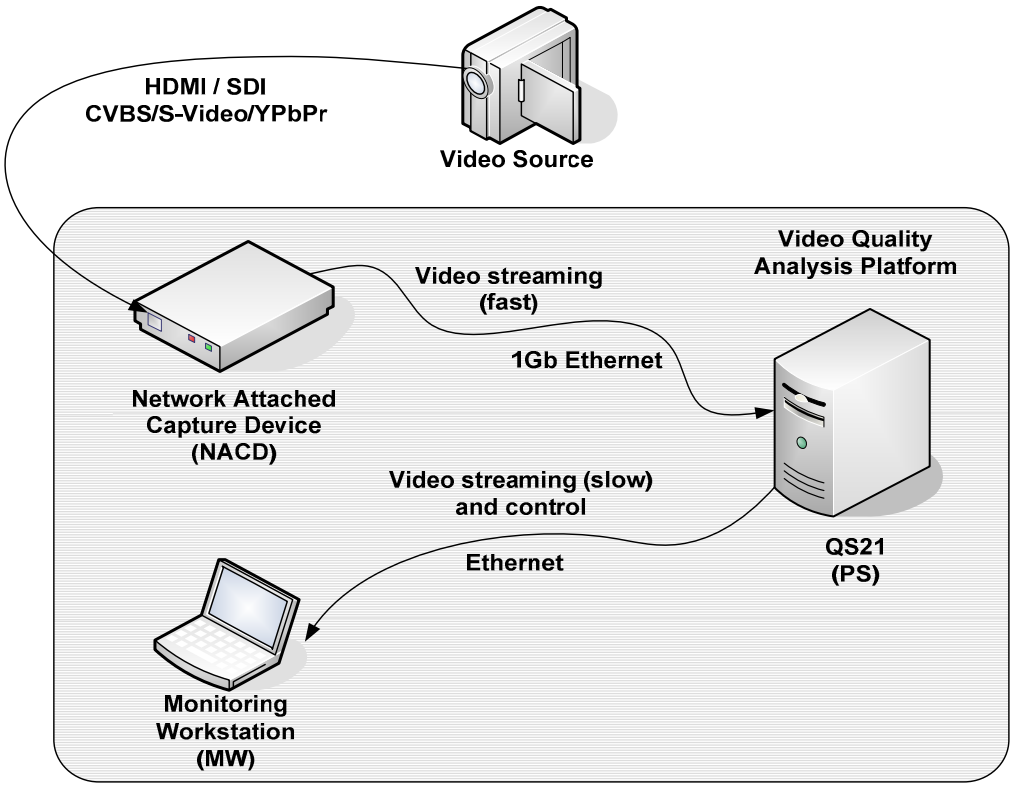

Fig 8. Architecture of the real-time VQA platform

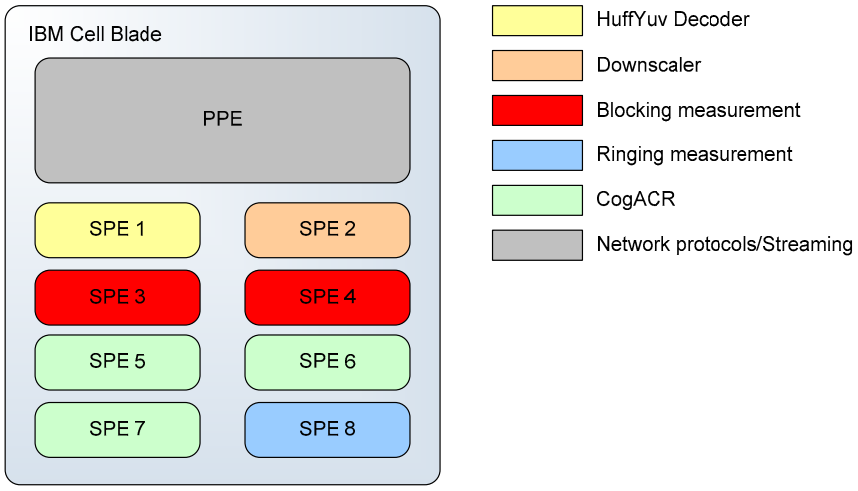

Fig 9. Task allocation in the improved VQA scheme with added CogACR blur assesment.